Engineering the organic semiconductor-electrode interface in polymer solar cells

Enrique D. Gomez*[a] and Yueh-Lin Loo*[b]

Received 14th January 2010, Accepted 11th March 2010
DOI: 10.1039/c000718h

Engineering the interfaces between organic semiconductors and electrodes minimizes interfacial resistances and enhances the performance of polymer solar cells. Organic semiconductors have intrinsically low free carrier densities, which can lead to large injection barriers if the work functions of the electrodes are not properly matched to the energy levels of the photoactive layers in electronic devices. One approach to engineer this crucial interface is through the judicious selection of electrode materials. Selecting the electrodes so their work functions match the energy levels of the organic semiconductors within the photoactive layer, however, can often compromise the environmental stability of polymer solar cells. One must thus strive to achieve a balance during device fabrication between the bulk properties of the electrode, such as electrical conductivity, and its interfacial properties, such as the energy alignment between the organic semiconductor and the electrode. Another approach to enhance charge extraction at the organic semiconductor-electrode interface is to adsorb molecular layers (MLs) on the electrode prior to the deposition of the photoactive layer. If the adsorbed molecules are preferentially oriented and they possess a net dipole moment, MLs can be utilized to modify the work function of the electrode so to minimize resistive losses during charge extraction. In this approach, one needs to take into account changes in the morphology of the photoactive layer – which undoubtedly also alters device performance – that result due to differences in the surface energy of the ML-modified electrode. As an alternative to completely replacing the electrode, interfacial modification *via* ML adsorption offers optimization of the charge extraction efficacy at the organic semiconductor-electrode interface independent of the bulk conductivity of the electrode.

Introduction

Polymer solar cells are an emerging class of devices that promise to generate renewable power inexpensively.[1–4] Specifically, the use of solution-processed polymer organic semiconductors with inexpensive fabrication methods, such as ink-jet printing and roll-to-roll processing, can lead to low-cost photovoltaic

[a]*Department of Chemical Engineering, The Pennsylvania State University, University Park, PA, 16802, USA. E-mail: edg12@psu.edu*
[b]*Department of Chemical Engineering, Princeton University, Princeton, NJ, 08544, USA. E-mail: lloo@princeton.edu*

Enrique D. Gomez

Professor Enrique D. Gomez received his B.S. in Chemical Engineering from the University of Florida and his Ph.D. in Chemical Engineering from the University of California, Berkeley. After a year and a half as a postdoctoral research associate at Princeton University, he joined the faculty at the Chemical Engineering Department of the Pennsylvania State University in August of 2009.

Yueh-Lin Loo

Yueh-Lin (Lynn) Loo is an associate professor in the Chemical Engineering Department at Princeton University. She received bachelor's degrees in chemical engineering and in materials science and engineering from the University of Pennsylvania and her doctoral degree from Princeton University. Loo's research centers on developing patterning tools for organic electronic devices, and on understanding structure-function relationships in organic electrically-active materials. Her work in organic electronics has garnered numerous honors, most recently the 2010 John H. Dillon Medal from the American Physical Society.

devices.[5–7] Wide-spread commercialization, however, requires an improvement in the light-to-energy conversion efficiency,[8] currently at around 6% for state-of-the-art devices.[9] In a yet more recent press release, Solarmer has reported efficiencies as high as 7.9% for bulk heterojunction polymer solar cells.[10] These efficiencies, however, pale in comparison with the theoretical values predicted for organic and polymer devices.[11,12] This review focuses on one specific aspect of the community's efforts to improve device performance through engineering of the organic semiconductor-electrode interface, both to minimize contact resistances and to control the morphology of the subsequently deposited photoactive layer.[1,13–18]

To generate high levels of current or current density in polymer solar cells, the barrier for charge transport across the organic semiconductor-electrode interface should be minimized. Ignoring surface dipoles, the barrier for charge transport across the organic semiconductor-electrode interface is proportional to the difference between the energy level of the highest occupied molecular orbital (HOMO) and the work function of the anode or the energy level of the lowest unoccupied molecular orbital (LUMO) and the cathode work function. Charge transport across the potential barrier occurs either through thermal excitation of carriers over the barrier or by tunneling through the barrier. Although the migration of free carriers in the organic semiconductor to the interface narrows the barrier width and promotes tunneling of charges through the barrier,[19] undoped organic semiconductors, have few, if any, free carriers.[20] It is thus crucial that electrodes are designed to match either the energy level of the HOMO of organic semiconductors having p-characteristics to maximize hole transport across the organic semiconductor-electrode interface, or the energy level of the LUMO of organic semiconductors with n-characteristics to maximize electron transport. As described next, the photoactive layer in polymer solar cells comprise at least two organic semiconductors, one which exhibits p-characteristics and the other n-characteristics, necessitating a cathode and an anode with different work functions.

The photoactive layer in bulk-heterojunction polymer solar cells is composed of a blend of an electron donor (organic semiconductor having p-characteristics) and an electron acceptor (organic semiconductor having n-characteristics). A schematic of such a device and its relevant energy levels are shown in Fig. 1. After photon capture, an exciton, or a tightly bound electron-hole pair, is generated; excitons that diffuse to the interface between the two organic semiconductors then separate into free charge carriers. Charge separation into the respective phases is driven by the difference in the LUMO energy levels of the organic semiconductors when light absorption takes place in the electron donor and is also driven by the difference in the HOMO energy levels when light absorption takes place in both constituents; generally a difference of 300–500 meV is thought to be required for this process to occur efficiently.[21] The carriers then migrate towards their respective electrodes, where the charges are extracted from the photoactive layer. The overall device efficiency is thus dictated by the product of efficiencies associated with these individual processes. Extensive research has shown that efforts to optimize the efficiency of any one of these processes frequently come at the expense of the efficiency of other processes. In polymer solar cells that utilize electron donors with HOMO energy levels near −5 eV, such as poly(3-hexylthiophene) (P3HT), high work function electrodes, such as indium tin oxide (ITO) or gold, are used as anodes to match the HOMO energy level of the electron donor to facilitate hole extraction.[3,8] When electron acceptors with LUMO energy levels around −4 eV, such as phenyl-C_{61} butyric acid methyl ester (PCBM), are used, low work function electrodes, such as Al or Ca, are necessary to match the LUMO energy levels.[22–30] Al and Ca, however, are susceptible to oxidation given their low electron affinities. When oxidized, Al and Ca suffer a significant reduction in electrical conductivity. As a consequence, polymer solar cells having Al or Ca as cathodes suffer device failure upon exposure to air. Such devices are therefore generally fabricated and tested in an inert atmosphere. Subtle but equally important is the surface energy of the electrode as it can alter the morphology of the subsequently deposited photoactive layer, ultimately influencing device performance.[17,18,31,32] Consequently, while the selection of an electrode whose work function matches the energy level of the organic semiconductor can minimize the barrier for charge extraction, it can simultaneously alter the morphology of the photoactive layer, thereby negatively influencing device operation.

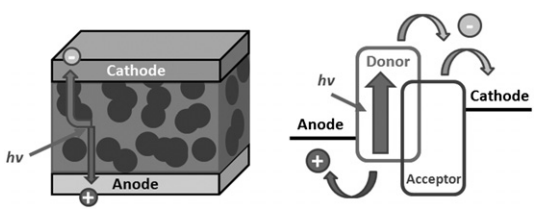

Fig. 1 Schematic of the architecture (left) and energy levels (right) of a bulk-heterojunction polymer solar cell. Although light absorption can take place in either the electron donor or electron acceptor, photoabsorption by the electron donor is illustrated in this figure.

An alternative approach to replacing the electrode entirely is to optimize the properties of the organic semiconductor-electrode interface by adsorbing molecular layers at the interface.[13,14,33–36] The deposition of preferentially aligned molecular layers can alter the work function of the electrode through the introduction of a net dipole at the electrode surface.[37–43] This approach decouples the bulk properties of the electrode, such as conductivity and environmental stability, from its surface properties, such as work function. By selecting the appropriate molecular layer, both the open-circuit voltage (V_{OC})[13] and the short-circuit current density (J_{SC})[13,14,35,44] can be improved in polymer solar cells. As our library of organic semiconductor continues to increase, interfacial engineering—optimization of electrode surface properties independent of bulk properties—will play an increasingly important role in enabling the implementation of novel materials having drastically different electrical characteristics.

This review focuses on recent efforts in engineering the organic semiconductor-electrode interface in polymer solar cells to decrease interfacial resistances and improve device performance. We begin with a discussion on the selection of electrodes that can maximize charge extraction at the organic semiconductor-electrode interface—often at the expense of other important properties. The second half of our review focuses on tuning the work functions and surface energies of the electrodes *via* molecule

adsorption. Specifically, we highlight recent efforts to minimize contact resistances in polymer solar cells through adsorbed molecular layers and recent progress aimed at elucidating the role that the electrode surface energy has on the composition of the subsequently deposited photoactive layer along the depth of the film.

Exploring the role of energy level matching at the organic semiconductor-electrode interface through judicious electrode selection

Selecting the proper electrode to optimize the organic semiconductor-electrode interface can be critical for the operation of polymer solar cells. For example, the effect of utilizing different cathode materials has been explored for polythiophene-based and polyphenylenevinylene-based polymer solar cells.[16,45] Fig. 2 shows the open cell voltage (V_{OC}), fill factor (FF) and normalized efficiency for P3HT/PCBM bulk-heterojunction polymer solar cells with cathodes having different work functions (ϕ_m). Changing the cathode material from silver ($\phi_m = -4.3$ eV) to barium ($\phi_m = -2.7$ eV) resulted in a 200 meV increase in the V_{OC}

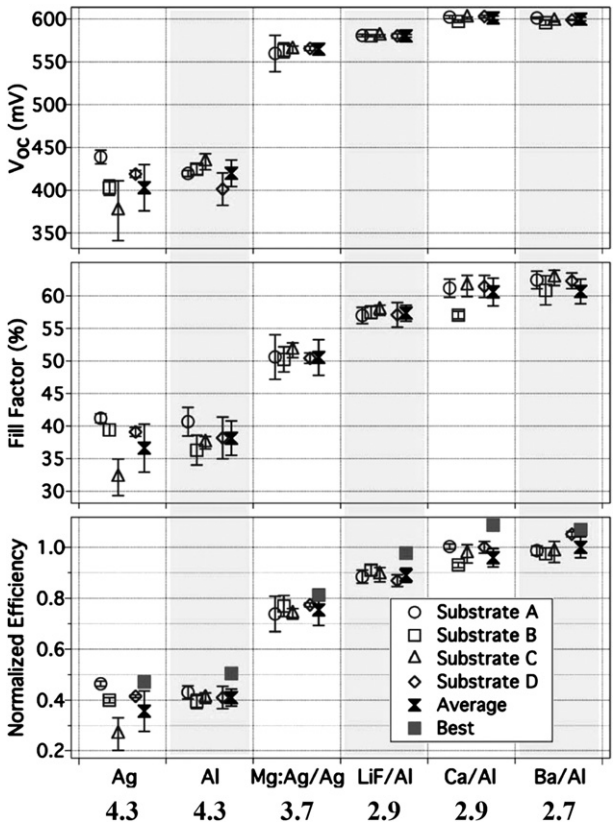

Fig. 2 The influence of cathode work function on the V_{OC}, fill factor and normalized efficiency of P3HT/PCBM (1 : 1 by weight) polymer solar cells. Average values are displayed both for individual and groups of substrates. Highest values obtained (best) are also shown. Error bars denote plus and minus one standard deviation. The work functions of the cathodes are listed below the cathode labels in eV. With the exception of the LiF/Al cathode (0.6 nm LiF/100 nm Al), all composite cathodes are cast as 20 nm of the first material listed and 80–100 nm for the second. (Reproduced with permission from ref. 16, © 2008, American Institute of Physics).

of the corresponding devices. In addition, the fill factor monotonically increases with decreasing cathode work function. Another study, in which mixtures of poly(2-methoxy-5-(3′,7′-dimethyloctyloxy)-*p*-phenylene vinylene) (MDMO-PPV) and PCBM are contacted with Pd ($\phi_m = -5.1$ eV), Au (−5.1 eV), Ag (−4.3 eV), or LiF/Al (−2.9 eV) as the cathode, also reported an increase in the V_{OC} with decreasing work function of the cathode.[45] In the case of the LiF/Al cathode, LiF is used as a thin interfacial layer (~1 nm) between the photoactive layer and the Al cathode. Since LiF is an insulator, it is kept thin to minimize resistive losses.[46] Utilizing a low work function cathode (>−4 eV), such as the LiF/Al combination, enables the extraction of electrons from the LUMO of PCBM while minimizing interfacial resistances at the organic semiconductor-cathode interface. In both of the examples above, however, electrodes with work functions that match the LUMO energy level of PCBM (*ca.* −4 eV) also have low electron affinities and are therefore susceptible to oxidation. Devices constructed with such cathodes uniformly suffer from poor device stability when they are exposed to air and are thus only stable when constructed and tested in an inert atmosphere.

Unlike silicon-based solar cells in which metal grids commonly serve as electrodes, organic and polymer solar cells—which utilize organic semiconductors with low charge mobilities compared to Si—require the use of transparent electrodes that allow simultaneous photon penetration to the photoactive layer and charge extraction. The necessity of a transparent electrode for polymer solar cells has led to the widespread use of ITO. Given its work function (−4.2 to −4.7 eV depending on processing conditions),[47–50] however, the use of ITO as an anode leads to large interfacial resistance at the hole transfer interface with many polymer electron donors having HOMO energy levels of approximately −5 eV.[49–52] Consequently a 50–100 nm film of poly(3,4-ethylenedioxythiophene) that is doped with poly(styrenesulfonate), PEDOT:PSS, is often introduced as a hole-transport layer between ITO and the photoactive layer in polymer solar cells. The work function of commercially available PEDOT:PSS (Clevios P by H.C. Starck, for example) is between −4.8 and −5.0 eV; its presence thus provides better energy level alignment for hole extraction from polymer electron donors to ITO.[53–55] The importance of energy level alignment at the organic semiconductor-anode interface was explored by Frohne and coworkers; they systematically modified the work function of PEDOT:PSS films electrochemically.[15,56] First, films of PEDOT were electrochemically polymerized from ethylenedioxythiophene on ITO. Then, the PEDOT films were subjected to various potentials in the presence of sodium-neutralized PSS (NaPSS), leading to PEDOT:PSS films with work function variations up to 1.3 eV, depending on the doping level.[56] The authors utilized the PEDOT:PSS films as hole-transport layers in MDMO-PPV/PCBM solar cells and tracked the compensation voltage, V_0 (the potential at which the photocurrent equals the dark current), as a function of the PEDOT:PSS work function.[15] V_0 is proportional to the V_{OC}. As seen in Fig. 3, V_0 of polymer solar cells tracks the work function of PEDOT:PSS. However, as the PEDOT:PSS work function continues to increase beyond 0.3 V versus Ag/AgCl, V_0 plateaus. The saturation in V_0 occurs as the work function of PEDOT:PSS approaches the HOMO level of the polymer electron donor, where the barrier for charge

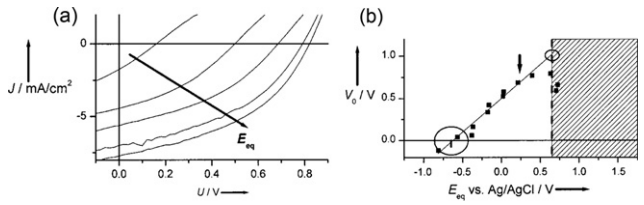

Fig. 3 (a) *J-V* characteristics of MDMO-PPV/PCBM (1 : 4 by weight) polymer solar cells incorporating modified PEDOT:PSS with various work functions as the hole-transport layer. Device performance improves with increasing work function of PEDOT:PSS (E_{eq}). (b) Crossover voltage, V_0, as a function of modified PEDOT:PSS work function. The arrow denotes data taken from a device utilizing commercially available PEDOT:PSS. In the gray region the work function of PEDOT:PSS is higher than the first oxidation potential of MDMO-PPV. (Reproduced with permission from ref. 15, © 2002, Wiley-VCH).

transport across the MDMO-PPV/anode interface is minimized.[15]

The necessity of using PEDOT:PSS as a hole-transport layer for ITO anodes in polymer solar cells represents a compromise between optimizing properties that are important at the organic semiconductor-electrode interface and those of the bulk electrode. Unfortunately, the poor conductivity of commercially available PEDOT:PSS (~1 S/cm) does not allow PEDOT:PSS to function alone as the anode, as the series resistance would drastically decrease device short circuit current density.[57] Recent efforts, however, have improved the conductivity of polymer acid doped conductive polymers, such as PEDOT:PSS[57–61] and polyaniline doped with poly(2-acrylamido-2-methyl-1-propanesulfonic acid) (PANI:PAAMPSA).[62–64] These efforts have led to the implementation of polymer-only anodes, resulting in polymer solar cells with similar device performance to devices with ITO/PEDOT:PSS anodes.[57,65,66] Given the scarcity of ITO and its increasing costs, the ability to replace ITO/PEDOT:PSS anodes with polymer-only anodes represents one significant advance towards the production of low-cost polymer solar cells.

As exemplified by the use of PEDOT:PSS to facilitate the transport of holes from the photoactive layer to the anode, energy level alignment in polymer solar cells can be greatly enhanced through the introduction of thin carrier transport layers at the organic semiconductor-electrode interfaces.[3,14,33–35,67,68] The implementation of thin electron-transport or hole-transport layers to enhance charge transfer across the photoactive layer-cathode and photoactive layer-anode interfaces, respectively, is well established in the organic light-emitting diode community.[69–73] Borrowing on this concept, thin layers of amorphous titanium oxide (TiOx) have been introduced on ITO to facilitate electron transfer in polymer solar cells. The energy level of the conduction band of TiOx is well matched with the LUMO energy level of PCBM (*ca.* −4 eV), allowing TiOx to serve as an electron-transport layer. However, the energy level of the valence band of TiOx is −7.5 eV, effectively blocking holes from the photoactive layer.[14,67,74,75] After TiOx deposition, the organic semiconductor blend is then deposited on top of the TiOx layer to form the photoactive layer. Finally, Au is deposited on top of the photoactive layer as the anode, creating an "inverted" polymer solar cell architecture in which electrons, instead of holes, are collected at the ITO electrode. A schematic comparing the architectures of conventional and inverted polymer solar cells can be found in Fig. 4a. Since TiOx does not have a high conductivity (~0.1 S/cm),[76] electron-transport layers comprising TiOx are deliberately kept thin (*ca.* 50 nm) to minimize series resistances within the device.[67] Other electron transport layers, such as zinc oxide, conjugated polyelectrolytes, and viologen doped with cobaltocene, have also been utilized in polymer solar cells.[68,77–80] Through insertion of materials with appropriate work functions as the electron-transport layers, the *J-V* characteristics and the overall device efficiencies of inverted solar cells are now comparable to those of conventional solar cells, as seen in Fig. 4b. The replacement of easily oxidized electrodes such as Al and Ca in inverted polymer solar cells also provide the added advantage of dramatically enhanced air stability.[67]

In the examples highlighted so far, the properties of the charge transfer interface in polymer solar cells are optimized by utilizing a completely different electrode material or by introducing a separate interfacial layer. Although the insertion of thin films of low-conductivity materials, such as LiF, TiOx, or PEDOT:PSS, allows optimization of the electrode surface without severe penalties to the bulk properties of the electrode, these layers still have drawbacks. LiF, for example, is highly hygroscopic. PSS is acidic and can slowly leach indium from ITO. Titania has shallow traps; devices comprising titania thus exhibit transient photovoltaic behavior.[81] These phenomena, though not always detrimental, can complicate device operation. As such, recent research on interfacial engineering in polymer

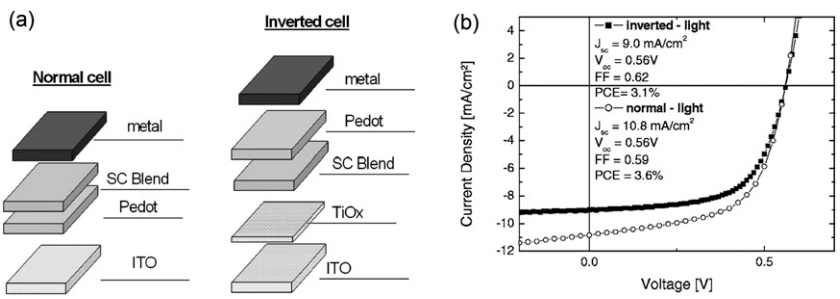

Fig. 4 (a) Comparison of conventional (normal) and inverted solar cell architectures. SC blend stands for organic semiconductor blend, and Pedot for PEDOT:PSS. (b) *J-V* characteristics under 1 sun illumination of conventional (normal) and inverted P3HT/PCBM (0.9 : 1 by weight) polymer solar cells. The J_{SC}, V_{OC}, fill factor and efficiency for both conventional and inverted cells are shown in the inset of the figure. (Reproduced with permission from ref. 67, © 2006, American Institute of Physics).

solar cells explores the deposition of molecular layers at the electrode surface instead. Similar to the utilization of thin layers at the organic semiconductor-electrode interface described above, the insertion of molecular layers allows independent control of the charge transfer interface without affecting the bulk properties of the electrode. Unlike the thin layers at the organic semiconductor-electrode interface, however, these molecular layers are frequently only several nanometers thick comprising molecules that are chemically adsorbed on the electrode. In the next section we will focus on this approach of engineering the charge extraction interfaces in polymer solar cells.

Interfacial modification using molecular layers to facilitate charge extraction from the photoactive layer

Interfacial modification through molecular layer adsorption is a novel direction in engineering the organic semiconductor-electrode interface not yet widely studied in polymer solar cells. Preferentially oriented molecular assemblies or self-assembled monolayers (SAMs) that are deposited on electrodes can have net dipoles that are capable of changing the work functions of substrates.[13,14,33–37,40,82,83] By controlling the dipole of the molecular layers through the judicial selection of chemical functionality and molecular architecture, the work function of the electrode can be, in principle, modified by more than 1 eV.[39,43] Furthermore, deposition of molecular layers can alter the surface energy of the metal electrode.[82,84,85] Consequently, SAMs adsorption on electrodes enables the tuning of both the work function and the surface energy of the electrode without altering the bulk properties of the metal electrode. Such an approach to interfacial engineering thus decouples the interfacial and bulk properties of the electrode, allowing for exquisite engineering of the organic semiconductor-electrode interface independent from the rest of the electrode.

Engineering of the organic semiconductor-electrode interface through molecular layer adsorption at the cathode has been performed on inverted polymer solar cells.[14,35] For example, Fig. 5a shows a schematic of the device architecture of an inverted solar cell employing a C60 carboxylic acid molecular layer at the interface between zinc oxide (ZnO; the cathode) and the P3HT/PCBM photoactive layer. The inset in Fig. 5a shows the chemical structure of the C60 carboxylic acid derivative that is deposited on ZnO. Fig. 5b shows the *J-V* characteristics of inverted solar cells with and without the C60 carboxylic acid adlayer between ZnO and the photoactive layer. The stability of inverted solar cells under ambient conditions is also highlighted in Fig. 5b where the *J-V* characteristics are compared between solar cells processed in ambient and inert conditions.[35] The increase in the device J_{SC} (by about 33%) due to the deposition of C60 carboxylic acid on ZnO is clear in Fig. 5b. The deposition of a variety of carboxylic acids (terthiophene, benzoic and lauric) on TiOx also leads to improved device efficiencies, up to 35%.[14] As exemplified in Fig. 5b, the improvement in efficiency is largely due to an improvement in the J_{SC} and FF while the V_{OC} is unchanged.[14,35] Contrary to what is expected of molecular layer adsorption on electrodes, the V_{OC} remains largely constant and this suggests that the adlayer does not alter the work function of the cathode significantly. The lack of work function modification may be due to a lack of a large dipole on the molecule. Instead, the improvement in the J_{SC} is attributed to a decrease in the contact resistance through markedly reduced charge recombination events at the organic semiconductor-cathode interface, and perhaps the reduction of the number of shunt paths.[35]

Molecular layers have also been used on the organic semiconductor-anode interface in conventional polymer solar cells.[13] Silane molecules, for example, have been deposited on ITO. Preferential orientation of the molecular within the adlayer leads to a net dipole which serves to alter the work function of the electrode. A variety of SAMs, N-propyltriethoxysilane (C-SAM) and aminopropyl triethoxysilane (N-SAM) comprising electron-donating hydrocarbon moieties and trichloro(3,3,3-trifluoropropylsilane) (F-SAM) comprising electron-withdrawing characteristics, were deposited on ITO. Through secondary electron emission spectroscopy, the deposition of C-SAM and N-SAM was found to lower the work function of ITO, from −4.7 eV to −3.9 eV and −4.4 eV, respectively, while the deposition of F-SAM raised the work function of ITO to −5.2 eV.[13] Surprisingly, the deposition of all three molecules on ITO led to an increase in the device V_{OC} when compared to polymer solar cells made with bare ITO. As seen in Fig. 6, the V_{OC}s of devices with SAM-treated ITO (between 0.55 and 0.60 V) are uniformly greater than the V_{OC} of devices with untreated ITO (0.36 V). Interestingly, the V_{OC} of N-SAM- and C-SAM-treated devices is similar to that of ITO devices prior to thermal annealing; the V_{OC} of these devices only increases with annealing at 150 °C for 20 min. In contrast, the V_{OC} of ITO devices decreases slightly with annealing. Although there is no concrete explanation at this time for the non-intuitive dependence of the V_{OC} with surface

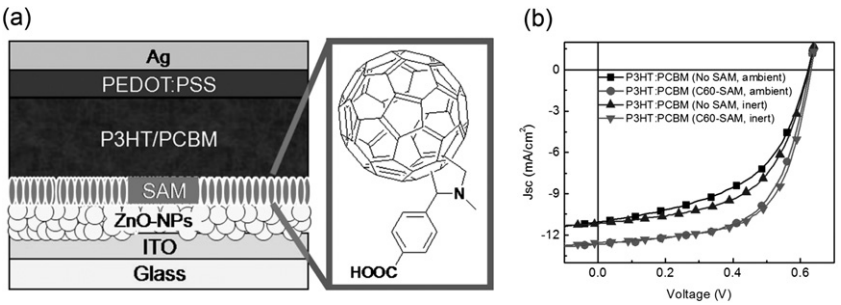

Fig. 5 (a) Schematic of device architecture of an inverted polymer solar cell employing C60 carboxylic acid modified cathode. (b) *J-V* characteristics of inverted ZnO NP/P3HT/PCBM (1 : 0.6 by weight) polymer solar cells with and without C60-carboxylic acid modification processed under inert and ambient conditions. (Reproduced with permission from ref. 35, © 2008, American Institute of Physics).

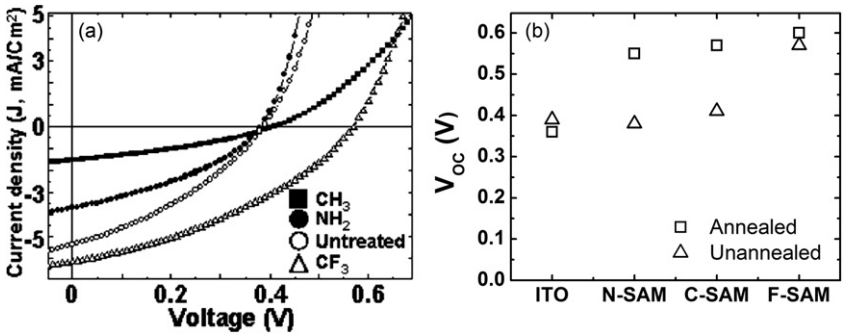

Fig. 6 (a) *J-V* characteristics of P3HT/PCBM (1 : 1 by weight) polymer solar cells built with various silane-modified ITO anodes. CH_3 stands for C-SAM in the text, NH_2 for N-SAM, CF_3 for F-SAM, and untreated for ITO-only devices. Devices were annealed at 150 °C for 20 min. (b) V_{OC} of unannealed devices and devices annealed at 150 °C for 20 min built with various SAM-modified ITO anodes. Note that the V_{OC} is always higher for devices modified with molecular layers at the organic semiconductor-anode interface. (Reproduced with permission from ref. 13, © 2007, American Institute of Physics).

modification, changes in the V_{OC} with processing conditions imply significant structural rearrangement in the photoactive layers that are in contact with anodes having drastically different surface energies when the devices are subjected to thermal annealing. In this case, perhaps changes in morphology dominate over changes in the work function. Blends of two or more chemically incompatible species should spontaneously phase separate. Thermal annealing provides additional molecular motion to the constituents; coarsening of phase-separated domains is typically reported with extended annealing of polymer blends. Complicating this issue further is the fact that the photoactive layers are generally only several hundreds of nanometers thick so their phase separation characteristics can be heavily influenced by the surface energies of the substrates onto which they are deposited. In our final section, we will highlight recent efforts in elucidating such changes in the structure of the photoactive layer, focusing on morphological evolution due to changes in the surface energy of the electrode.

Controlling the electrode surface energy and vertical phase separation of the photoactive layer through the implementation of molecular layers

In addition to tuning the electronic properties of the electrode, molecular layers can also modify the surface energy of the electrode,[82,84,85] and consequently affect the vertical composition profile of the photoactive layer.[17,18,31,32,86] The thin-film photoactive layer in polymer solar cells is on the order of 100 nm thick, and consequently is susceptible to significant composition fluctuations along the depth of the film due to the surface energy of the substrate. Campoy-Quiles and coworkers used variable-angle spectroscopic ellipsometry (VASE) to determine the PCBM concentration as a function of depth of P3HT/PCBM films cast on quartz and on hexamethyldisilazane-modified Si.[18] The concentration profiles extracted from modeling of the VASE data are shown in Fig. 7. By decreasing the surface energy (going from the hydrophilic quartz surface to the hydrophobic SAM-treated Si surface), the compositions as a function of film depth change dramatically. Fig. 7 shows that the PCBM concentration at the organic semiconductor-substrate interface is depleted when the photoactive layer is deposited on SAM-modified Si instead of quartz. These experiments suggest that PCBM preferentially segregates to the hydrophilic surface, presumably due to the polar nature of the ester group. Often termed vertical phase separation, compositional heterogeneities along the depth of the film are a direct consequence of the different surface energies at the bottom and top of the photoactive layer. Xu and coworkers used XPS to examine the composition at the top and bottom of P3HT/PCBM films cast on glass, as well as those on PEDOT:PSS and Cs_2CO_3.[17] The bottom of the films was accessed by lifting off the film in water. Consistent with work by Campoy-Quiles *et al.*, Xu *et al.* found that PCBM tends to segregate to hydrophilic surfaces, such as glass and Cs_2CO_3. Depending on the processing conditions, the PCBM concentration at the photoactive layer-substrate interface can be 4 to 10 times the concentration at the top surface of the photoactive layer.[17]

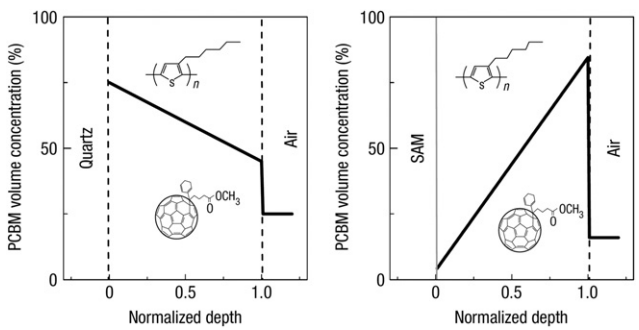

Fig. 7 PCBM concentration determined using VASE as a function of depth of P3HT/PCBM (1 : 1 by weight) films deposited on either quartz (hydrophilic substrate) or hexamethyldisilazane-treated Si (SAM, hydrophobic substrate). (Reprinted with permission from ref. 18, © 2008, Nature Publishing Group).

Given that the bottom electrode generally serves as the anode to collect holes during device operation, preferential segregation of PCBM at the anode is undesirable as it leads to higher recombination losses and consequently lower device performance. Despite numerous efforts to examine the extent of vertical phase separation through a variety of techniques, such as electron microscopy, Rutherford backscattering spectroscopy, nuclear reaction analysis, and secondary ion mass spectroscopy, no clear relationship exists between the extent of vertical phase separation and device performance.[17,18,24,30,32,87–93] This challenge

in large part stems from the morphological complexities of bulk-heterojunction photoactive layers.[94] In addition to composition fluctuations along the depth of the photoactive layer induced by differences in surface energies, the organic semiconductors are sufficiently chemically different that they have a strong tendency to phase separate in the lateral direction of the photoactive layer as well. Further complicating structural development is the tendency for such highly conjugated organic semiconductors to crystallize.

The decoupling of vertical phase separation from lateral phase separation and crystallization is thus complex. The deposition of molecular layers at the electrode surface provides another way to alter the morphology of the photoactive layer by changing the surface energy. This approach is fundamentally different from changing annealing conditions or casting solvents during device fabrication as the modification of surface energies alters the thermodynamic driving force for vertical phase separation. By controlling thermodynamic parameters as opposed to kinetic parameters,[95] the processing history dependence of the photoactive layer morphology can be deemphasized, leading to more robust and predictable device performance.

Summary and outlook

Engineering of the organic semiconductor-electrode interface is critical for high-performance polymer solar cells. The utilization of the well-established approach of implementing thin layers at the organic semiconductor-electrode interface to improve energy level alignment, originally developed for organic light emitting diodes, has led to significant improvement of device performance in polymer solar cells. The implementation of molecular layers at the electrode surface allows for separate control of interfacial and bulk properties of the electrode. As an independent parameter, the surface energy can also be tuned through the deposition of molecular layers, with direct, observable consequences to the vertical phase separation of the organic semiconductor photoactive layer. The complexity of the multiple-length scale, three-dimensional structural development within the photoactive layer, however, has so far overwhelmed our attempts to fully elucidate structure-function relationships in polymer solar cells.

As our library of organic semiconductors continues to grow, the challenge remains to develop strategies for the successful implementation of novel materials in polymer solar cells. The polymer photovoltaic field continues to push for low-band gap materials and electron acceptors with higher LUMO levels, thus increasing the necessity to engineer the electrical properties of organic semiconductor-electrode interfaces to achieve high-performance devices. New organic semiconductors will not necessarily have the same interaction energies as existing systems, such as P3HT and PCBM, and hence, may exhibit drastically different phase separation characteristics. Consequently, engineering the organic semiconductor-electrode interface through molecular layer adsorption may be critical for us to generate the know-how to process these new materials. The ability to tune both the work function and surface energy will allow for some independent control of electronic and morphological properties, possibly enabling optimization of organic photoactive materials independent of electrode selection.

Acknowledgements

MRSEC funding through Princeton's NSF-sponsored Princeton Center for Complex Materials is acknowledged. Funding from the Sloan Foundation and the Photovoltaics Program at the Office of Naval Research is also acknowledged.

References

1 S. E. Shaheen, D. S. Ginley and G. E. Jabbour, *MRS Bull.*, 2005, **30**, 10–19.
2 H. Hoppe and N. S. Sariciftci, *Adv. Polym. Sci.*, 2008, **214**, 1–86.
3 B. C. Thompson and J. M. J. Frechet, *Angew. Chem., Int. Ed.*, 2008, **47**, 58–77.
4 G. Li, V. Shrotriya, Y. Yao, J. S. Huang and Y. Yang, *J. Mater. Chem.*, 2007, **17**, 3126–3140.
5 H. Yan, Z. H. Chen, Y. Zheng, C. Newman, J. R. Quinn, F. Dotz, M. Kastler and A. Facchetti, *Nature*, 2009, **457**, 679–686.
6 H. Sirringhaus, T. Kawase, R. H. Friend, T. Shimoda, M. Inbasekaran, W. Wu and E. P. Woo, *Science*, 2000, **290**, 2123–2126.
7 C. J. Brabec, J. A. Hauch, P. Schilinsky and C. Waldauf, *MRS Bull.*, 2005, **30**, 50–52.
8 G. Dennler, M. C. Scharber and C. J. Brabec, *Adv. Mater.*, 2009, **21**, 1323–1338.
9 J. Y. Kim, K. Lee, N. E. Coates, D. Moses, T. Q. Nguyen, M. Dante and A. J. Heeger, *Science*, 2007, **317**, 222–225.
10 www.solarmer.com, accessed on December 2009.
11 G. Dennler, M. C. Scharber, T. Ameri, P. Denk, K. Forberich, C. Waldauf and C. J. Brabec, *Adv. Mater.*, 2008, **20**, 579.
12 M. C. Scharber, D. Wuhlbacher, M. Koppe, P. Denk, C. Waldauf, A. J. Heeger and C. L. Brabec, *Adv. Mater.*, 2006, **18**, 789–794.
13 J. S. Kim, J. H. Park, J. H. Lee, J. Jo, D. Y. Kim and K. Cho, *Appl. Phys. Lett.*, 2007, **91**, 112111.
14 S. K. Hau, H. L. Yip, O. Acton, N. S. Baek, H. Ma and A. K. Y. Jen, *J. Mater. Chem.*, 2008, **18**, 5113–5119.
15 H. Frohne, S. E. Shaheen, C. J. Brabec, D. C. Muller, N. S. Sariciftci and K. Meerholz, *ChemPhysChem*, 2002, **3**, 795–799.
16 M. O. Reese, M. S. White, G. Rumbles, D. S. Ginley and S. E. Shaheen, *Appl. Phys. Lett.*, 2008, **92**, 053307.
17 Z. Xu, L. M. Chen, G. W. Yang, C. H. Huang, J. H. Hou, Y. Wu, G. Li, C. S. Hsu and Y. Yang, *Adv. Funct. Mater.*, 2009, **19**, 1227–1234.
18 M. Campoy-Quiles, T. Ferenczi, T. Agostinelli, P. G. Etchegoin, Y. Kim, T. D. Anthopoulos, P. N. Stavrinou, D. D. C. Bradley and J. Nelson, *Nat. Mater.*, 2008, **7**, 158–164.
19 S. M. Sze, *Semiconductor Devices: Physics and Technology*, John Wiley and Sons, Inc., New York, 2002.
20 W. Brutting, ed., *Physics of organic semiconductors*, Wiley-VCH, New York, 2005.
21 B. Kippelen and J. L. Bredas, *Energy Environ. Sci.*, 2009, **2**, 251–261.
22 M. C. Scharber, D. Wuhlbacher, M. Koppe, P. Denk, C. Waldauf, A. J. Heeger and C. L. Brabec, *Adv. Mater.*, 2006, **18**, 789.
23 Y. Kim, S. Cook, S. M. Tuladhar, S. A. Choulis, J. Nelson, J. R. Durrant, D. D. C. Bradley, M. Giles, I. McCulloch, C. S. Ha and M. Ree, *Nat. Mater.*, 2006, **5**, 197–203.
24 J. K. J. van Duren, X. N. Yang, J. Loos, C. W. T. Bulle-Lieuwma, A. B. Sieval, J. C. Hummelen and R. A. J. Janssen, *Adv. Funct. Mater.*, 2004, **14**, 425–434.
25 H. Spanggaard and F. C. Krebs, *Sol. Energy Mater. Sol. Cells*, 2004, **83**, 125–146.
26 H. Hoppe and N. S. Sariciftci, *J. Mater. Res.*, 2004, **19**, 1924–1945.
27 K. M. Coakley and M. D. McGehee, *Chem. Mater.*, 2004, **16**, 4533–4542.
28 N. S. Sariciftci, D. Braun, C. Zhang, V. I. Srdanov, A. J. Heeger, G. Stucky and F. Wudl, *Appl. Phys. Lett.*, 1993, **62**, 585–587.
29 P. W. M. Blom, V. D. Mihailetchi, L. J. A. Koster and D. E. Markov, *Adv. Mater.*, 2007, **19**, 1551–1566.
30 H. Hoppe, M. Niggemann, C. Winder, J. Kraut, R. Hiesgen, A. Hinsch, D. Meissner and N. S. Sariciftci, *Adv. Funct. Mater.*, 2004, **14**, 1005–1011.
31 M. P. Felicissimo, D. Jarzab, M. Gorgoi, M. Forster, U. Scherf, M. C. Scharber, S. Svensson, P. Rudolf and M. A. Loi, *J. Mater. Chem.*, 2009, **19**, 4899–4901.

32 D. S. Germack, C. K. Chan, B. H. Hamadani, L. J. Richter, D. A. Fischer, D. J. Gundlach and D. M. DeLongchamp, *Appl. Phys. Lett.*, 2009, **94**, 233303.
33 H. L. Yip, S. K. Hau, N. S. Baek, H. Ma and A. K. Y. Jen, *Adv. Mater.*, 2008, **20**, 2376–2382.
34 H. L. Yip, S. K. Hau, N. S. Baek and A. K. Y. Jen, *Appl. Phys. Lett.*, 2008, **92**, 193313.
35 S. K. Hau, H. L. Yip, H. Ma and A. K. Y. Jen, *Appl. Phys. Lett.*, 2008, **93**, 233304.
36 S. Khodabakhsh, B. M. Sanderson, J. Nelson and T. S. Jones, *Adv. Funct. Mater.*, 2006, **16**, 95–100.
37 D. M. Alloway, M. Hofmann, D. L. Smith, N. E. Gruhn, A. L. Graham, R. Colorado, V. H. Wysocki, T. R. Lee, P. A. Lee and N. R. Armstrong, *J. Phys. Chem. B*, 2003, **107**, 11690–11699.
38 B. H. Hamadani, D. A. Corley, J. W. Ciszek, J. M. Tour and D. Natelson, *Nano Lett.*, 2006, **6**, 1303–1306.
39 G. Heimel, L. Romaner, E. Zojer and J. L. Bredas, *Nano Lett.*, 2007, **7**, 932–940.
40 S. Khodabakhsh, D. Poplavskyy, S. Heutz, J. Nelson, D. D. C. Bradley, F. Murata and T. S. Jones, *Adv. Funct. Mater.*, 2004, **14**, 1205–1210.
41 W. Chen, C. Huang, X. Y. Gao, L. Wang, C. G. Zhen, D. C. Qi, S. Chen, H. L. Zhang, K. P. Loh, Z. K. Chen and A. T. S. Wee, *J. Phys. Chem. B*, 2006, **110**, 26075–26080.
42 R. Rousseau, V. De Renzi, R. Mazzarello, D. Marchetto, R. Biagi, S. Scandolo and U. del Pennino, *J. Phys. Chem. B*, 2006, **110**, 10862–10872.
43 G. Heimel, L. Romaner, E. Zojer and J. L. Bredas, *Acc. Chem. Res.*, 2008, **41**, 721–729.
44 T. C. Monson, M. T. Lloyd, D. C. Olson, Y. J. Lee and J. W. P. Hsu, *Adv. Mater.*, 2008, **20**, 4755.
45 V. D. Mihailetchi, P. W. M. Blom, J. C. Hummelen and M. T. Rispens, *J. Appl. Phys.*, 2003, **94**, 6849–6854.
46 C. J. Brabec, S. E. Shaheen, C. Winder, N. S. Sariciftci and P. Denk, *Appl. Phys. Lett.*, 2002, **80**, 1288–1290.
47 D. J. Milliron, I. G. Hill, C. Shen, A. Kahn and J. Schwartz, *J. Appl. Phys.*, 2000, **87**, 572–576.
48 F. Nuesch, L. J. Rothberg, E. W. Forsythe, Q. T. Le and Y. L. Gao, *Appl. Phys. Lett.*, 1999, **74**, 880–882.
49 Y. Park, V. Choong, Y. Gao, B. R. Hsieh and C. W. Tang, *Appl. Phys. Lett.*, 1996, **68**, 2699–2701.
50 K. Sugiyama, H. Ishii, Y. Ouchi and K. Seki, *J. Appl. Phys.*, 2000, **87**, 295–298.
51 J. S. Kim, M. Granstrom, R. H. Friend, N. Johansson, W. R. Salaneck, R. Daik, W. J. Feast and F. Cacialli, *J. Appl. Phys.*, 1998, **84**, 6859–6870.
52 Y. Yi, J. E. Lyon, M. M. Beerbom and R. Schlaf, *J. Appl. Phys.*, 2006, **100**, 093719.
53 T. M. Brown, J. S. Kim, R. H. Friend, F. Cacialli, R. Daik and W. J. Feast, *Appl. Phys. Lett.*, 1999, **75**, 1679–1681.
54 G. Greczynski, T. Kugler, M. Keil, W. Osikowicz, M. Fahlman and W. R. Salaneck, *J. Electron Spectrosc. Relat. Phenom.*, 2001, **121**, 1–17.
55 J. S. Huang, P. F. Miller, J. S. Wilson, A. J. de Mello, J. C. de Mello and D. D. C. Bradley, *Adv. Funct. Mater.*, 2005, **15**, 290–296.
56 H. Frohne, D. C. Muller and K. Meerholz, *ChemPhysChem*, 2002, **3**, 707–711.
57 J. Y. Kim, J. H. Jung, D. E. Lee and J. Joo, *Synth. Met.*, 2002, **126**, 311–316.
58 B. Y. Ouyang, C. W. Chi, F. C. Chen, Q. F. Xi and Y. Yang, *Adv. Funct. Mater.*, 2005, **15**, 203–208.
59 X. Crispin, S. Marciniak, W. Osikowicz, G. Zotti, A. W. D. Van der Gon, F. Louwet, M. Fahlman, L. Groenendaal, F. De Schryver and W. R. Salaneck, *J. Polym. Sci., Part B: Polym. Phys.*, 2003, **41**, 2561–2583.
60 S. K. M. Jonsson, J. Birgerson, X. Crispin, G. Greczynski, W. Osikowicz, A. W. D. van der Gon, W. R. Salaneck and M. Fahlman, *Synth. Met.*, 2003, **139**, 1–10.
61 J. Ouyang, Q. F. Xu, C. W. Chu, Y. Yang, G. Li and J. Shinar, *Polymer*, 2004, **45**, 8443–8450.
62 J. E. Yoo, T. L. Bucholz, S. Y. Jung and Y.-L. Loo, *J. Mater. Chem.*, 2008, **18**, 3129–3135.
63 J. E. Yoo, J. L. Cross, T. L. Bucholz, K. S. Lee, M. P. Espe and Y.-L. Loo, *J. Mater. Chem.*, 2007, **17**, 1268–1275.
64 J. E. Yoo, K. S. Lee, A. Garcia, J. Tarver, E. D. Gomez, K. Baldwin, Y. Sun, H. Meng, T.-Q. Nguyen and Y.-L. Loo, *Proc. Natl. Acad. Sci. U. S. A.*, 2010, **107**, 5712–5717.
65 F. L. Zhang, M. Johansson, M. R. Andersson, J. C. Hummelen and O. Inganas, *Adv. Mater.*, 2002, **14**, 662–665.
66 S. I. Na, S. S. Kim, J. Jo and D. Y. Kim, *Adv. Mater.*, 2008, **20**, 4061.
67 C. Waldauf, M. Morana, P. Denk, P. Schilinsky, K. Coakley, S. A. Choulis and C. J. Brabec, *Appl. Phys. Lett.*, 2006, **89**, 233517.
68 C. S. Kim, S. Lee, L. L. Tinker, S. Bernhard and Y.-L. Loo, *Chem. Mater.*, 2009, **21**, 4583–4588.
69 H. Aziz and Z. D. Popovic, *Appl. Phys. Lett.*, 2002, **80**, 2180–2182.
70 J. Blochwitz, M. Pfeiffer, T. Fritz and K. Leo, *Appl. Phys. Lett.*, 1998, **73**, 729–731.
71 L. S. Hung and C. H. Chen, *Mater. Sci. Eng., R*, 2002, **39**, 143–222.
72 A. P. Kulkarni, C. J. Tonzola, A. Babel and S. A. Jenekhe, *Chem. Mater.*, 2004, **16**, 4556–4573.
73 J. Park, C. V. Hoven, R. Q. Yang, N. S. Cho, H. B. Wu, T. Q. Nguyen and G. C. Bazan, *J. Mater. Chem.*, 2009, **19**, 211–214.
74 J. Y. Kim, S. H. Kim, H. H. Lee, K. Lee, W. L. Ma, X. Gong and A. J. Heeger, *Adv. Mater.*, 2006, **18**, 572.
75 C. Y. Li, T. C. Wen, T. H. Lee, T. F. Guo, J. C. A. Huang, Y. C. Lin and Y. J. Hsu, *J. Mater. Chem.*, 2009, **19**, 1643–1647.
76 R. G. Breckenridge and W. R. Hosler, *Phys. Rev.*, 1953, **91**, 793–802.
77 S. K. Hau, H. L. Yip, N. S. Baek, J. Y. Zou, K. O'Malley and A. K. Y. Jen, *Appl. Phys. Lett.*, 2008, **92**, 253301.
78 M. T. Lloyd, R. P. Prasankumar, M. B. Sinclair, A. C. Mayer, D. C. Olson and J. W. P. Hsu, *J. Mater. Chem.*, 2009, **19**, 4609–4614.
79 D. C. Olson, Y. J. Lee, M. S. White, N. Kopidakis, S. E. Shaheen, D. S. Ginley, J. A. Voigt and J. W. P. Hsu, *J. Phys. Chem. C*, 2008, **112**, 9544–9547.
80 J. Luo, H. B. Wu, C. He, A. Y. Li, W. Yang and Y. Cao, *Appl. Phys. Lett.*, 2009, **95**, 043301.
81 C. S. Kim, S. S. Lee, E. D. Gomez, J. B. Kim and Y.-L. Loo, *Appl. Phys. Lett.*, 2009, **94**, 113302.
82 S. A. Paniagua, P. J. Hotchkiss, S. C. Jones, S. R. Marder, A. Mudalige, F. S. Marrikar, J. E. Pemberton and N. R. Armstrong, *J. Phys. Chem. C*, 2008, **112**, 7809–7817.
83 S. R. Saudari, P. R. Frail and C. R. Kagan, *Appl. Phys. Lett.*, 2009, **95**, 023301.
84 P. E. Laibinis and G. M. Whitesides, *J. Am. Chem. Soc.*, 1992, **114**, 1990–1995.
85 A. Noy, C. D. Frisbie, L. F. Rozsnyai, M. S. Wrighton and C. M. Lieber, *J. Am. Chem. Soc.*, 1995, **117**, 7943–7951.
86 A. Kumar, G. Li, Z. R. Hong and Y. Yang, *Nanotechnology*, 2009, **20**, 165202.
87 A. M. Higgins, S. J. Martin, R. L. Thompson, J. Chappell, M. Voigt, D. G. Lidzey, R. A. L. Jones and M. Geoghegan, *J. Phys.: Condens. Matter*, 2005, **17**, 1319–1328.
88 H. Hoppe, T. Glatzel, M. Niggemann, A. Hinsch, M. C. Lux-Steiner and N. S. Sariciftci, *Nano Lett.*, 2005, **5**, 269–274.
89 H. Hoppe, T. Glatzel, M. Niggemann, W. Schwinger, F. Schaeffler, A. Hinsch, M. C. Lux-Steiner and N. S. Sariciftci, *Thin Solid Films*, 2006, **511–512**, 587–592.
90 T. Martens, J. D'Haen, T. Munters, Z. Beelen, L. Goris, J. Manca, M. D'Olieslaeger, D. Vanderzande, L. De Schepper and R. Andriessen, *Synth. Met.*, 2003, **138**, 243–247.
91 X. Yang and J. Loos, *Macromolecules*, 2007, **40**, 1353–1362.
92 S. S. van Bavel, E. Sourty, G. de With and J. Loos, *Nano Lett.*, 2009, **9**, 507–513.
93 B. V. Andersson, A. Herland, S. Masich and O. Inganas, *Nano Lett.*, 2009, **9**, 853–855.
94 S. S. Lee and Y.-L. Loo, *Annu. Rev. Chem. Biochem. Eng.*, 2010, **1**, 59.
95 C. S. Kim, L. L. Tinker, B. F. DiSalle, E. D. Gomez, S. Lee, S. Bernhard and Y.-L. Loo, *Adv. Mater.*, 2009, **21**, 3110–3115.